

Humidity Robustness of IGBT Guard Ring Termination

Charalampos Papadopoulos¹, Boni Boksteen¹, Gontran Pâques¹, Chiara Corvasce¹

¹ABB Semiconductors, Switzerland

Corresponding author: Boni Boksteen, Boni.Boksteen@ch.abb.com

The Power Point Presentation will be available after the conference

Abstract

IGBT power semiconductor modules are used in various high power applications including traction, industrial drives, grid systems and renewables such as in wind-power generation, conversion and automotive. Many of these applications are subject to harsh environmental conditions and in particular, when the inverter cabinets do not shield the power electronics, including the IGBT modules, from such conditions. Therefore, IGBT modules can be exposed to severe humidity levels. In this paper, we investigate the influence of the combination of humidity and high voltage on the blocking reliability of IGBT devices with guard-ring terminations. An improved testing approach HV-H³TRB (High Temperature, High Humidity & High Voltage), when compared to classical THB (High Temperature, High Humidity & Biased) is applied to assess the robustness of different termination designs and passivation stacks. Full description of the failure mode and of its correlation to the humidity induced electrical field modifications is also provided. This analysis offers an insight on the design and testing aspects, which are of key importance to the development of environmentally robust high power IGBTs.

1. Introduction

Predicting the robustness of various power semiconductor designs for a planned lifetime of up to 30 years is very challenging, even more so since the conditions of the environmental impact are mostly not well understood. In many power electronics applications the IGBT modules are subject to harsh environmental conditions with severe humidity levels. Also, the temperature of the module can rise or drop relatively fast when the inverter is not always running under full load conditions, being idle or running in partial load. Additionally to a running system, often power semiconductor devices or the system itself are exposed to an ambient environment before getting installed and running. Based on the above discussed points, moisture can penetrate into the IGBT modules during long periods without any high temperature levels to drive out moisture from the modules. Another aspect is that condensation can appear while having a temperature drop during operation, which can lead to severe changes in the material properties (e.g. dielectric properties of chip passivation and module encapsulation materials such as silicone gel and polyimide). These undesirable modifications can have a negative impact on the electric field at the periphery of the

semiconductor device and therefore cause an increased localized stress at the chip junction termination region. Therefore, it is crucial that the materials used for an IGBT module and the design of the power semiconductor especially chip termination and passivation can cope with the increased stress levels. Recently more and more information about the capability of IGBTs and diodes have been shown [1,2,3] for a variety of termination concepts and the possibility to further improve the devices and their reliability.

1. Testing environmental robustness

In the past, the standard THB High Temperature, High Humidity & Biased test with 85% RH (relative humidity) and 85°C was used at a reverse bias voltage of 80V, with a typical test time requirement of 1000 hours representing a lifetime of 30 years. This test promotes charge or ion movements due to increased moisture levels combined with relatively higher temperatures and voltages, which allows detection of instabilities caused by process variations or insufficient design margins. With such a standard test, decades of experience have been accumulated. However, for high power semiconductors, the

80V applied reverse bias remains at a low level compared to typical voltages used in real power electronics converters. It was shown that by increasing the applied voltage to more realistic values [4,5], it is possible to accelerate corrosion by electrochemical mechanisms which could play a more dominant role during field operation when compared to the classical impact of charge or ion movement. In the presence of high electric fields and enough reactant moisture ions at the chip surface, electrochemical corrosion can occur causing several materials like aluminum, nitride and even oxide compositions to change their structure and lose the main protective functionality. Hence, the well-known HTRB (high temperature reverse bias) when not combined with moisture, is not representative to quantify the device performance operating in a harsh environment. A THB test with an increased collector emitter voltage, referred to as HV-H³TRB (i.e. High Voltage, High Humidity, High Temperature reverse biased) is the appropriate test to prove the robustness of the chip termination and passivation against humidity and high electric fields [3]. This test is typically performed in the standard controlled climatic environment and conditions of the well-established THB test while increasing the collector emitter voltage depending on the device voltage class up to 60 – 80% of the rated voltage.

2. The device under test (DUT)

In this paper we focus on the capability of a guard-ring termination design with metal field plates passivated by a semi insulating layer, silicon nitride and polyimide as shown in Fig. 1 - 3. To achieve a high level of humidity robustness for the applications previously discussed, major development steps are needed. In addition, taking typical device developments like reduced leakage currents, reduced termination width and thinned devices [6,7] into account makes the test even more challenging. These adaptations generally give less moisture resilience capability while causing increased electric fields in the termination and passivation at the required test conditions. Thus, while designing a termination including the passivation layers both, wet and dry condition needs to be taken into account through simulation and representative tests.

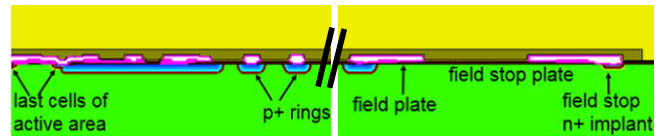


Fig. 1: Schematic TCAD cross-section of a guard-ring termination design. Highlighted areas of interest are the p+ rings (not all shown), field plate and field stop plate.

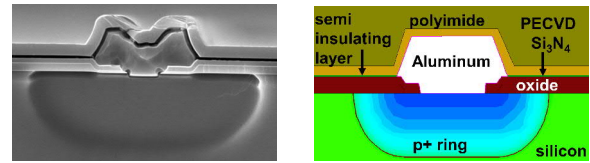


Fig. 2: Overview of a p+ ring with metal connection. On the left a SEM cross-section, on the right the corresponding TCAD structure detailing the passivation layers.

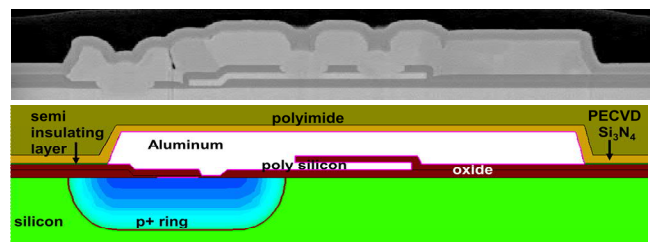


Fig. 3: Overview of a field plate of the termination design. On top a SEM cross-section of the field plate is shown. The bottom figure shows the corresponding TCAD structure detailing the poly silicon and metal field plate and its passivation layers.

3. The humidity impact on IGBT junction termination

This section discusses the junction termination designs of the investigated samples and provides a qualitative TCAD analysis of the humidity effect on the electric field distribution. To evaluate the possible changes in the electric field due to humidity exposure, the moisture absorption in the polyimide layer and the surrounding gel is accounted in simulation by an increased value of permittivity of a factor of 10 compared to a polyimide or gel without water content of a value of 3.4. Such an increase aims to represent the extreme case of having a water saturated layer as a water film directly in contact with the silicon nitride passivation. Fig. 4 illustrates the impact of dry and wet conditions and therefore increased permittivity of the ambient and of the polyimide layer while modifying the electric field distribution for the IGBT termination by simulating the whole termination/ passivation structure presented in Fig. 1. The cutline parallel to the two most critical electric field positions in the silicon nitride

layer shows the strong increase of the local electrical field peaks at each silicon ring location due to the increased permittivity of the polyimide and the ambient. The increase becomes larger when moving close to the active area, as shown in Fig. 5. A detailed zoom at the field plates is shown in Fig. 6 showing the impact on the termination and potential critical locations for designing a termination. The field peak strength remains comparable to the dry peak in most locations except between the field plates and towards the active area including the gate runner, where a larger region of high electric fields is generated. As a qualitative outcome of the simulation results, an increased humidity content in the ambient (or encapsulating material such as silicone gel) and in the polyimide is expected to cause a strengthening of the electric field in the silicon nitride layer in the proximity of the active area and in the field free zone towards the two field plates.

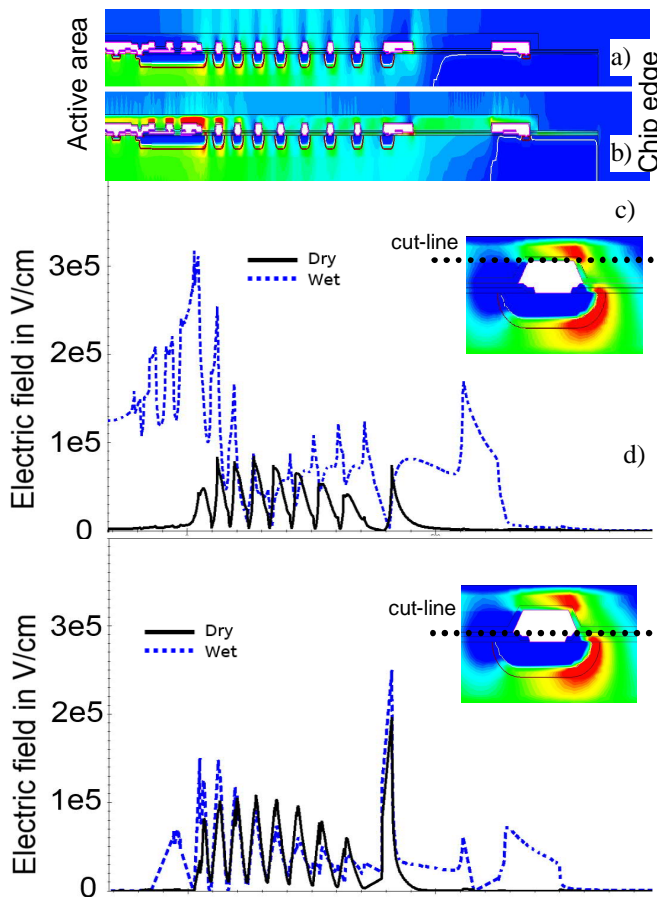


Fig. 4: a) Electric field contour plot of the 1.7kV IGBT simulation in reverse blocking at 1.3kV (overview picture) without water absorption, b) with water absorption and c) cutline of electric field at nitride on highest topology on aluminum and d) cutline of electric field at nitride on flat position.

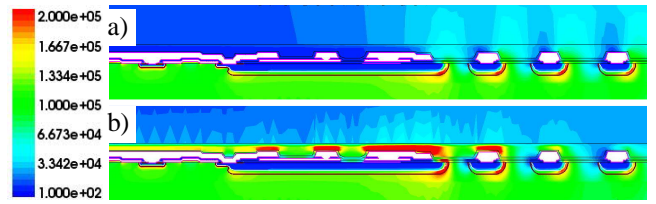


Fig. 5: a) Zoom of electric field contour plot of the 1.7kV IGBT simulation in reverse blocking at 1.3kV towards active area without water absorption and b) with water absorption.

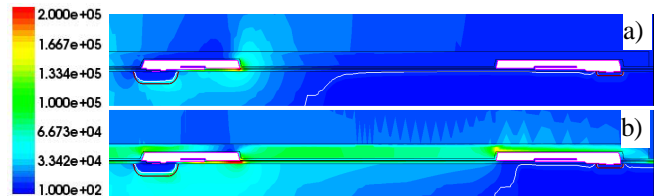


Fig. 6: a) Zoom of electric field contour plot of the 1.7kV IGBT simulation in reverse blocking at 1.3kV at the field plates without water absorption and b) with water absorption.

4. Experimental results

To experimentally assess the behavior of the IGBT termination under humidity and electric field stress, several HV-H³TRB tests have been performed. The tests were carried out on 1.7kV IGBTs chips using as a test vehicle the improved HiPak module [8] with 16 IGBTs. The conditions in the test were 85°C, 85% RH and 1.36kV (80% collector emitter voltage) up to 1000h while using the ramp up and ramp down specifications within the typical THB standards. By measuring the weight of the modules after the test in comparison to pre-test measurements as produced, has shown that there is still a high amount of moisture in the organic materials (housing, gel, and polyimide) of +3g.

4.1 Electrical characteristics

The test was performed with 4 modules with an overall amount of 64 IGBTs. The blocking voltage and the gate emitter leakage of all devices was measured before and after the test to check the functionality of the device and detect electrical parameter changes. The module phases were connected together in the test with a bus bar and the full module was tested and monitored while having gate emitter shorted. The leakage current monitored during the test time is shown in the Fig. 7. The device blocking characteristics at room temperature has been measured at defined time steps by interrupting the test, as

reported in Fig. 7. The static blocking results at 25°C over time indicated in Fig. 7 are summarized in Fig. 8.

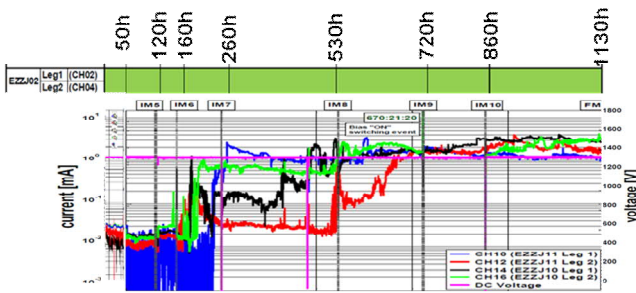


Fig. 7: Leakage current monitoring of a HV-H³TRB test at 1360V all 2 phases connected in parallel during the test. Each monitored color represents a module with 16 IGBTs.

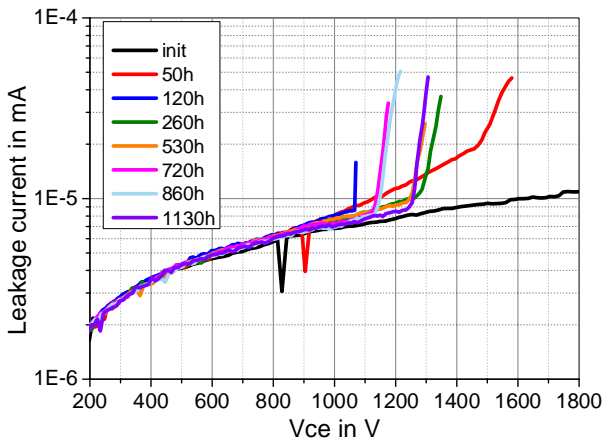


Fig. 8: Blocking voltage measurements at different time intervals of a representative HV-H³TRB stressed IGBT module phase at 25°C. In black before stress and the other colors post stress

All devices start to rise in leakage current after around 120 hours of stress which is the sign of a reduction of the blocking voltage below the applied DC voltage value of 1.36kV. However the leakage current is only a late indicator for the changes happening at the device level since a blocking capability reduction can be already detected after 50 hours. Though the leakage current rises, the devices still can run up to 1000h while reaching a balance with the moisture, visible in a stabilized leakage current. The generated heat from the increased leakage current slows down further humidity impact by reducing the moisture content at the termination. To better assess the impact of different electric field strengths, an additional test has been performed where the phases of 4 HiPak2 modules have been differently stressed with an

applied voltage of 900V, 1100V and 1360V. After the test the static blocking was measured to see the voltage dependency as shown in Fig. 9.

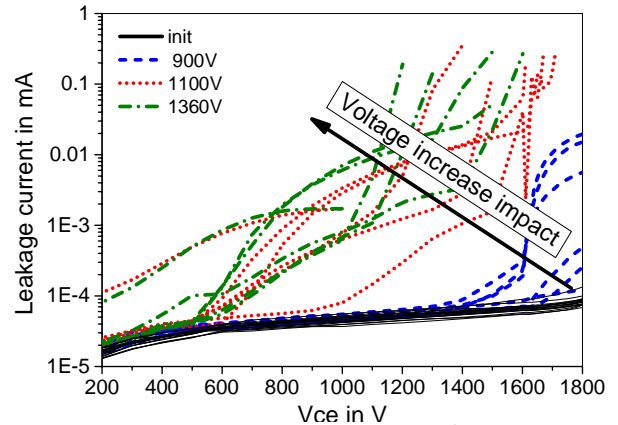


Fig. 9: Voltage dependency of HV-H³TRB test and shown blocking capability of each phase consisting each 8 IGBTs with initial performance in black of all phases, blue dashed with 900V, red dotted with 1100V and green dotted-dashed with 1360V with a stress time of 100h

It has to be noted that after the ramp down of the HV-H³TRB test no strong additional dry out procedure was applied. In fact, the blocking capability can be recovered if no device short or severe damage appeared during the test. Any further dry out procedure would allow the moisture trapped between layers to evaporate and thus to have no impact anymore on the device blocking capability. For demonstrating reason an additional dry-out of 24h at 125°C has been performed. The blocking characteristic comparison before and after is shown in Fig. 10.

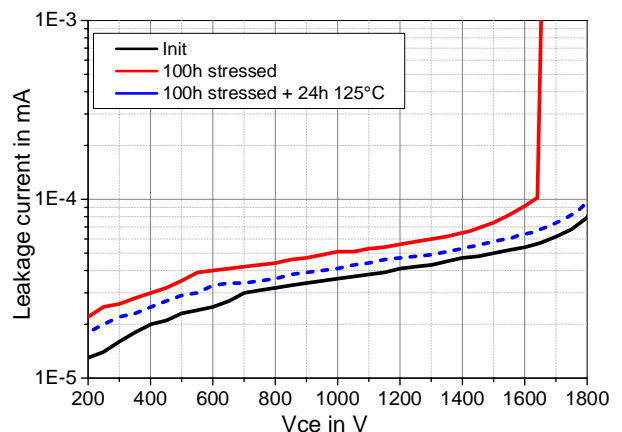


Fig. 10: Results of HV-H³TRB blocking capability of one phase with initial performance in black, reduced capability after 100h stress in red and with an oven dry out procedure of 24h at 125°C in dotted blue.

Therefore, the ramp down procedure and the time the stressed modules are stored in ambient before remeasuring is crucial to judge the humidity robustness of the device.

This type of static blocking recovery is not necessarily a statement that the device will be functional under switching conditions. During dynamic switching the electrical field peaks are stronger localized [9] in comparison to static blocking and enhanced by plasma modulation. As a consequence a small damage in the critical location can still cause device failure.

4.2 Failure analysis

4.2.1 Optical inspection

The tested samples have been analyzed under the microscope to investigate the root cause of device failure. For that the gel and housing have been removed. In all cases, all the chips show clear evidences of corrosion and polyimide delamination. The corroded regions are located as indicated by TCAD simulation shown in Fig. 4, 5 and 6. The positions correlate to the electric field peak locations, as illustrated in Fig. 11 and to the comparison to the electric field in Fig. 12. The direction of active area and termination edge is always kept as shown in the simulation structures.

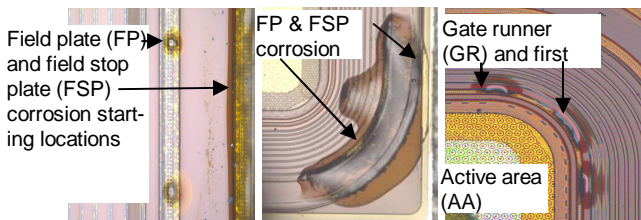


Fig. 11: IGBT optical inspection after module housing and gel removal. Left: test duration 50hours showing the termination region with the field plates and corrosion appeared in the field stop plate. Center and right after 1000h severe corrosion could be detected in the initial part of the termination. This corrosion is as simulated close to the gate runner and active area and on the region between the field plates at the edge of the chips. Polyimide delamination is visible. All chips corrode the same way, just more or less pronounced as indicated here with two IGBT pictures.

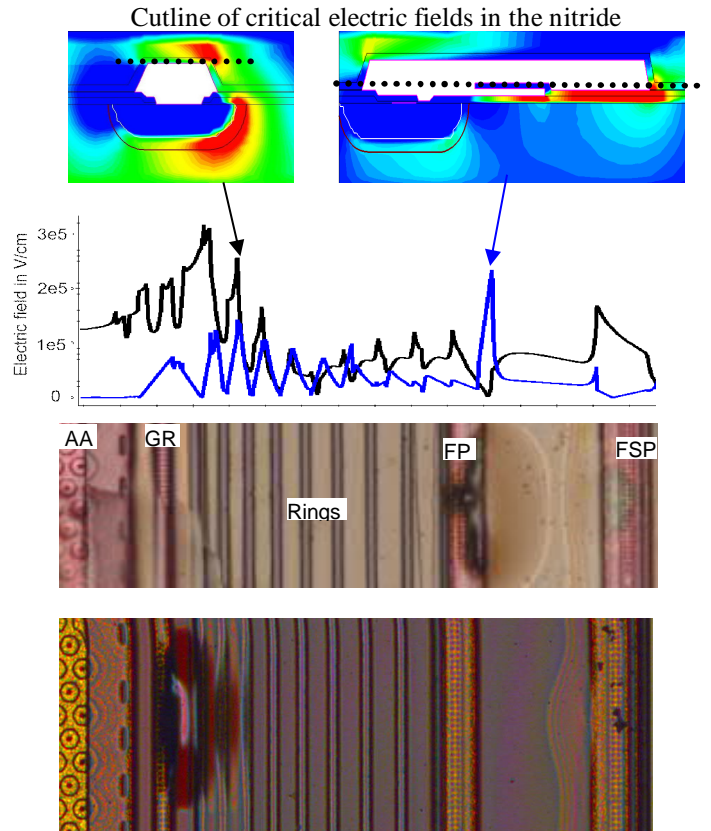


Fig. 12: Two examples of IGBT optical inspection defect locations compared to the two critical cuts from wet simulation fitting well to corrosion positions.

It is not given that the defect location is only where the high electric fields are located, they can also appear at other locations such as in the middle of the termination. However, there is a clear correlation showing that most of the degradation is in fact in the peak electric field locations, which is in accordance to the simulation study.

4.2.1 Focused Ion beam scanning electron microscopy (FIB-SEM)

To deepen the understanding of the corrosion mechanism a FIB-SEM analysis has been performed on the location of corrosion. The results are shown in Fig. 13, 14, 15. All the chips were analyzed without removing the polyimide to avoid any additional artefacts from preparation. The main evidences of the failure analysis are: lift-off of polyimide from the nitride surface, cracks of the nitride passivation layer, local structural changes of nitride and aluminum.

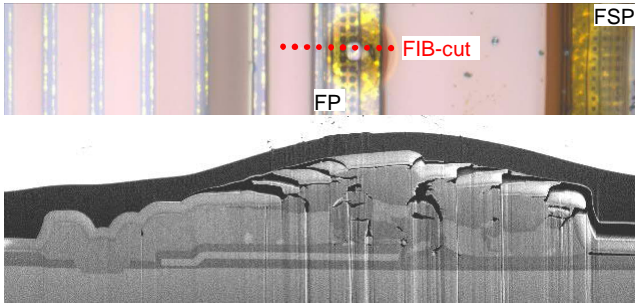


Fig. 13: Top optical microscopy defect location, bottom FIB-SEM picture of FP defect location as indicated by dotted line

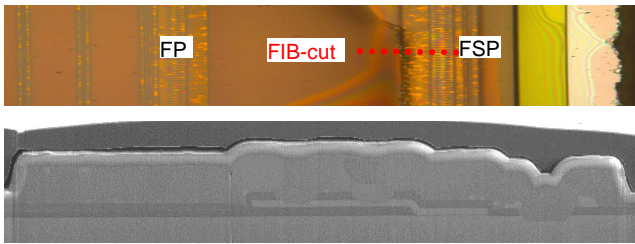


Fig. 14: Top optical microscopy defect location, bottom FIB-SEM picture of FPS defect location as indicated by dotted line

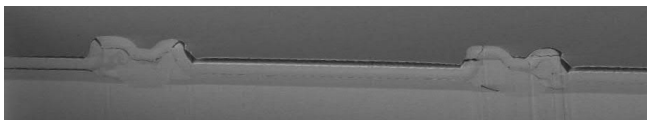
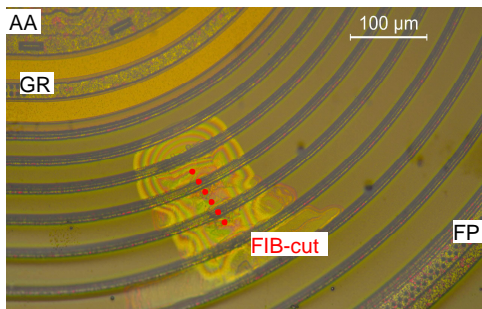


Fig. 15: Top optical microscopy defect location, bottom FIB-SEM picture of ring defect location as indicated by dotted line

The optical inspection without polyimide has revealed local spots on metal connection lines and traces of sparking between field plates, as shown in Fig. 16.



Fig. 16: Typical defects inspected by optical microscopy with removed polyimide, visible sparking between the plates on failed device and initial crack on the nitride

5. Failure mode interpretation

The failure analysis evidences support the interpretation of the possible failure mechanism as described in the following. After the chamber ambient is saturated at the defined humidity level, moisture penetrates into the module and silicone gel. The polyimide layer has a typical moisture uptake of less than 2% and it will be humidity saturated as well. As soon as enough reactant moisture reaches the nitride surface, corrosion of the nitride starts to appear enhanced by applied electric field, as reported by Osenbach in 1993 [10]. This corrosion is associated with electrochemical reactions based on the Frankel Poole conduction mechanism at the nitride surface. Additional reactants can either outgas [1,10] or trigger new reactions with the production of water of high PH value. The water acts aggressively against aluminum wherever no nitride protection is present by design or due to damaged nitride. The nitride reaction causes outgassing with high pressure at the polyimide interface resulting in a polyimide layer lift off. Hence, larger gaps appear in regions where the moisture can condense and cause further accelerated corrosion.

Spots of composition change from a uniform Si_3N_4 layer to a porous and brittle SiO_2 layer have been detected by energy dispersive x-ray spectroscopy (EDX) in the termination, as shown in Fig. 17.

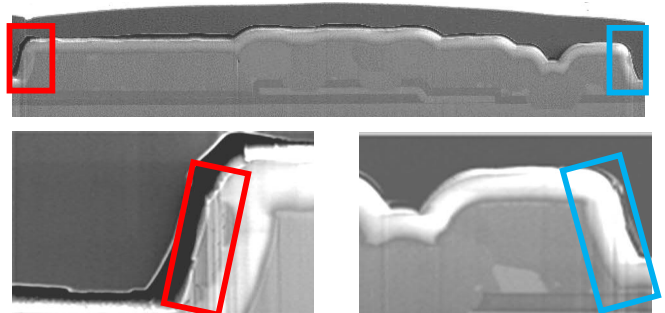


Fig. 17: FIB-SEM picture of initial corrosion on sidewall of PECVD Nitride layer and consequently lifted polyimide. Top the whole field plate and on the bottom the sidewalls on the two sides of the field plate

The spot locations correlate with the high electric field positions indicated from TCAD simulations. The porous layer is prone to crack enabling moisture to penetrate and reach the aluminum with consequent corrosion which can be even visually detected as color and structure volume change as can be seen in Fig. 13, 18 [11].

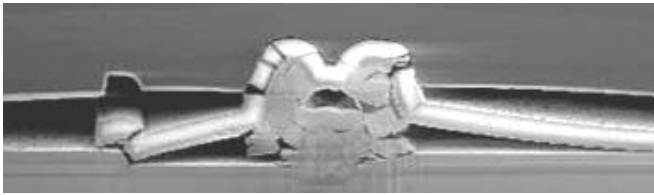


Fig. 18: FIB-SEM picture of aluminum corrosion and volume growth.

6. The improved passivation

As described previously, the nitride corrosion is the main degrading factor. It could be an approach to eliminate the nitride layer, but this is not a preferred option due to the protection capability of nitride layers against charges and mechanical damage. Another solution could be to change the nitride composition to a more stable nitride, as reported in [10,12]. However, these changes could have other drawbacks with higher reliability risks. Therefore, a preferred solution is to protect the nitride from a moisture environment or to delay the moisture penetration and in addition to protect the aluminum from contact with water.

This was achieved by using an improved polyimide on the nitride layer with reduced moisture uptake and an improved surface bond capability. Moreover, the semi insulating layer has been developed to act as additional moisture barrier, as shown in Fig. 19 where the structure of the old to new layer is compared.

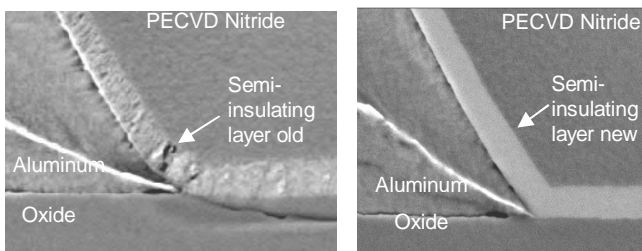


Fig. 19: SEM picture on a ring passivation zoomed into the semi insulating layer. Left: old layer allowing moisture to pass easily, right new layer acting as a barrier

Fig. 20 proves the stability of the leakage current over 1000 hours of HV-H³TRB test of the improved chip passivation. The IV blocking characteristics are compared before and after stress in Fig. 21 showing no change on aged devices. At the optical inspection of the measured samples no major corrosion effects are visible anymore as illustrated in Fig. 22.

Being no changes implemented in the packaging process and material, the performance achievements are only based on chip design improvements. Any change of packaging concept, process [13] and materials has to be newly investigated to quantify the impact on humidity robustness.

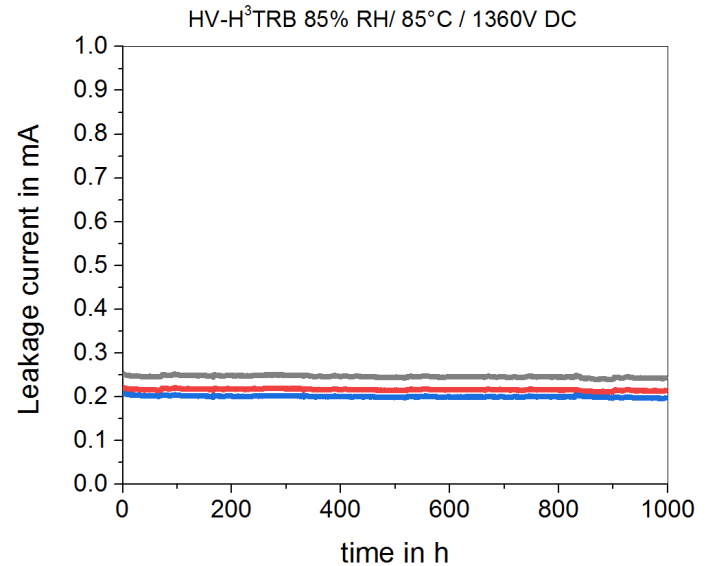


Fig. 20: Leakage current monitoring for the advanced passivation design concept for 3x fully populated HiPak2 modules with 24 IGBTs with an applied voltage of 1000h with a DC voltage of 1360V

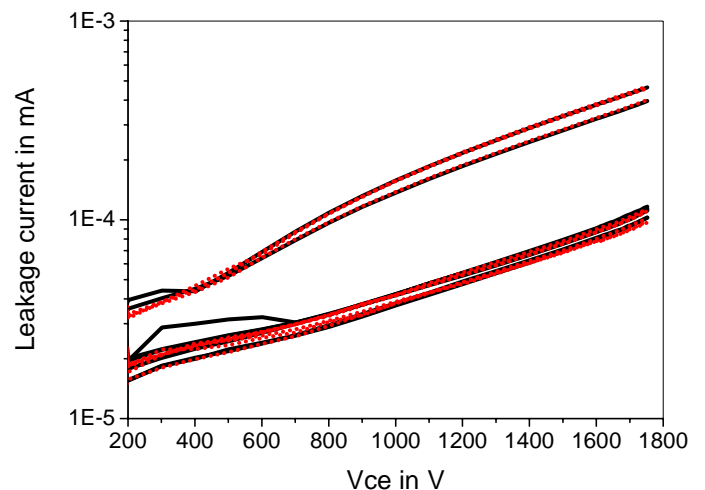


Fig. 21: IV measurements for the advanced passivation concept before and after HV-H³TRB at 1360V for 3x fully populated HiPak2 modules with 24 IGBTs. Black before stress and red dotted post stress measurement.

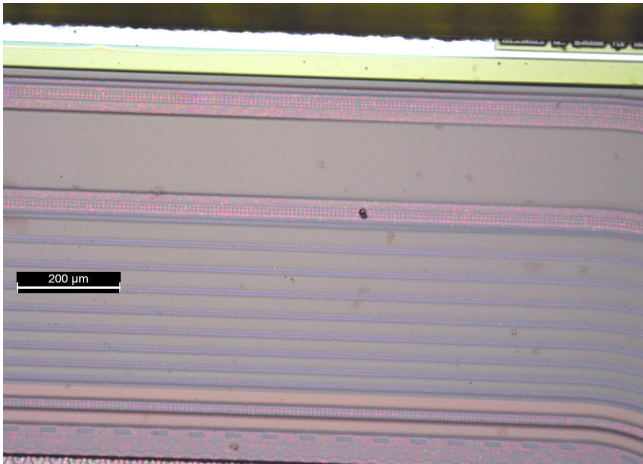


Fig. 22: Optical inspection of the advanced passivation concept. Optical inspection after module housing and gel removal. No major signs of degradation as previously reported.

7. Conclusions

The HV-H³TRB test sets a new standard for ensuring reliable operation of power devices. In this paper, we reported that nitride corrosion can appear during this test leading to accelerated degradation proven by many experimental showcases. This is mainly due to a material property change from nitride to silicon oxide resulting in further chemical reactions, out gassing and organic passivation adhesion loss. Additional generated reactants can also cause aluminum corrosion. The theory of corrosion and the corrosion positions could be correlated by detailed experimental layer analysis and simulations. The simulations enable to design improved terminations which are more robust to pass the HV-H³TRB test. Finally, we could show that there are options to pass the HV-H³TRB test with an improved polyimide and newly developed semi insulation layer without having any significant difference of pre to post measurements and no major signs of degradation in the final optical inspection.

ACKNOWLEDGEMENT

Special thanks to Munaf Rahimo for supporting as mentor, whose guidance and inspiration driving the thinking of to “B or not to B” enabling to reach a next level in device reliability.

The authors would like to thank R. Jabrany, G. Stampf, C. Toker-Bieri, P. Strasser, P. Kaspar S. Ninkovic, C. Widmer, G. Gunaratnam, L. Knezevic, K. Boucart, S. Rehm and C. Luhmann for the over all the years for the project and to have a major contribution realizing the many learning cycles leading to achieve the robust design.

Special thanks to N. Kaminski and C. Zorn for the Collaboration with University of Bremen supporting in testing and the discussions on the topic.

REFERENCES

- [1] C. Papadopoulos et. al., “The influence of humidity on the high voltage blocking reliability of power IGBT modules and means of protection”, ESREF 2018
- [2] O.Shilling et. al., “Humidity robustness for high voltage power modules: Limiting mechanisms and improvement of lifetime” ESREF 2018
- [3] N. Tanaka et al., “Robust HVIGBT module design against high humidity”, PCIM 2015, Nuremberg, 2015
- [4] C. Zorn, N. Kaminski, “Temperature Humidity Bias (THB) Testing on IGBT Modules at High Bias Levels”, Proc. International Conference on Integrated Power Systems (CIPS), Nuremberg, 2014
- [5] C. Zorn, N. Kaminski, “Acceleration of Temperature Humidity Bias (THB) Testing on IGBT Modules by High Bias Levels”, International Symposium on Power Semiconductor Devices and ICs (ISPSD), Hong Kong,
- [6] C. Corvasce et. al., “New 1700V SPT+ IGBT and Diode Chip Set with 175°C Operating Junction Temperature”, EPE 2011, Birmingham
- [7] C. Papadopoulos et. al., “The third generation 6.5kV HiPak2 module rated 1000A and 150°C”, PCIM2018 Nuremberg
- [8] G. Pâques et. al. “A new HiPak Module Platform with Improved Reliability”, PCIM2014 Nuremberg
- [9] B.K.Boksteen et. al.; “6.5 kV Field Shielded Anode (FSA) Diode Concept with 150C Maximum Operational Temperature Capability”, ISPSD’2018
- [10] J.W. Osenbach, “Water-Induced Corrosion of Materials Used for Semiconductor Passivation”, J. Electrochem. Soc., Vol140, No12, December 1993
- [11] Z. Xu et al., “Metal oxidation kinetics and the transition from thin to thick films”, Phys. Chem. Chem. Phys., 2012, 14, 14534–14539
- [12] T. Oku et al., “Moisture Resistance of Insulating Films for Compound Semiconductor Devices”, CS MANTECH Conference, May 19th - 22nd, 2014, Denver, Colorado, USA
- [13] M. Rahimo et. al. “The impact on power semiconductor device operation due to local electric field alterations in the junction termination region”, Microelectronics Journal, Reliability issues in Power Electronics, 2015